doi:10.1246/cl.2011.1201
Published on the web October 5, 2011

A New Composite Electrode of Li_2MnSiO_4 Nanoparticles Combined with Mesoporous Carbon CMK-3

Hideaki Yoshitake* and Takashi Kawase
Division of Materials Science and Chemical Engineering, Yokohama National University, 79-5 Tokiwadai, Hodogaya-ku, Yokohama, Kanagawa 240-8501

(Received July 1, 2011; CL-110554; E-mail: yos@ynu.ac.jp)

Li_2MnSiO_4 is prepared by nanocasting using CMK-3 mesoporous carbon, and its electrochemical behavior is explored without removing the CMK-3 template. This preparation provides a new cathode material for large capacity Li secondary batteries, equivalent to two-Li^+ charge–discharge processes.

Lithium orthosilicate Li_2MSiO_4 (where M = Mn, Fe, Co, or Ni) has recently attracted considerable attention due to its high theoretical capacity (ca. 330 mA h g^{-1}) when two Li^+ ions per formula are extracted in the electrochemical reactions of Li rechargeable batteries.[1–6] Interest in these oxides as potential cathode material for electric vehicles has been further promoted by their high cell voltage (3.1–4.3 V) due to the redox couples $Mn^{3+/4+}$, $Fe^{2+/3+}$, $Co^{3+/4+}$, and $Ni^{3+/4+}$ as well as ease of handling from a thermal stability perspective due to Si–O bonding. However, in addition to the low practical capacity that can be proved experimentally (ca. 120 mA h g^{-1}), low electroconductivity (10^{-12}–10^{-16} S cm^{-1}) has often been pointed out as a major disadvantage when they are compared with other cathode materials such as $LiCoO_2$ (10^{-4} S cm^{-1}), $LiMn_2O_4$ (10^{-6} S cm^{-1}), and $LiFePO_4$ (10^{-9} S cm^{-1}).

Recent sol–gel synthesis techniques have enabled us to provide much finer particles than by conventional preparation through solid-state reactions.[7–11] When using an organic acid such as citric acid as a complexing agent or an organic acid salt as the precursor, considerable amount of carbon can remain with the oxide particles, since the final stage of preparation of this mixed oxide is carried out under reducing conditions.[10,12–16] Acetylene black and glucose can also be used as the carbon source.[17,18] The coexistence of carbon coupled with the decrease in crystallite size can drastically enhance the electroconductivity and the capacity.[7,9,12,14,19] Although various structural analyses have been carried out using spectroscopic techniques,[11,15,19–21] in addition to microscopic observations,[7,16,20,21] the concentration, distribution, and structure of carbon and Li_2MSiO_4 are far from being optimized. This situation might be partly due to the difficulty in obtaining uniform structure of such complex electrode materials, especially at the mesoscopic level.

Apart from the conventional methods for molding electrodes, where carbon and oxide particles are bound or formed into core–shell particles, the dispersion of oxide particles in a carbon matrix with uniform mesopores and thin pore walls could be an alternative approach to elucidating the relationship between the electrochemical properties and the structure of the carbon and oxide particles. Mesoporous carbons that are prepared by nanocasting or supermolecular-templating methods[22–25] provide uniform mesopores, in which the size and the periodicity are usually controllable. Considering these structural features, periodically ordered mesoporous carbons are also expected to provide an excellent carbon matrix for model electrode materials from lithium orthosilicate–carbon composites. In this letter, we prepare Li_2MnSiO_4 nanoparticles in ordered mesoporous carbon CMK-3,[26] where the particles that are grown are up to the pore diameter in size, and we elucidate the electrochemical behavior in the charge–discharge reaction of Li ion.

CMK-3 was prepared according to the method developed by Ryoo et al.[26] The loading and dispersion of Li_2MnSiO_4 into the CMK-3 matrix was carried out via incipient-wetness and hydrolysis–condensation using citric acid and ethylene glycol (i.e., by the Pichini process). The precursors that were used for lithium, manganese, and silicon were lithium acetate, manganese acetate, and tetraethyl orthosilicate, respectively. The solutions were mixed with CMK-3, dried at 333 K, and then heated at 973 K under a 5% H_2-95% Ar gas mixture. The resulting solid is presented as LMSx@CMK-3, where x is the occupancy of the pores by Li_2MnSiO_4, which is calculated from the mixing ratio of the precursors and CMK-3. The detail procedure is provided in Electronic Supporting Information (ESI).[28]

Nitrogen adsorption–desorption experiments and X-ray diffraction were applied to confirm the structure of CMK-3, of which the isotherms, pore size distributions, and XRD pattern are depicted in ESI. Its BET surface area, pore size, and pore volume were 1431 m^2 g^{-1}, 2.5 and 5.0 nm (bimodal), and 1.17 mL g^{-1}, respectively. The pore volume decreased with increasing occupation of Li_2MnSiO_4: 0.57, 0.38, and 0.34 mL g^{-1} for LMS0.5@CMK-3, LMS1.0@CMK-3, and LMS1.5@CMK-3, respectively.

Figure 1 shows a typical transmission micrograph of LMSx@CMK-3. Parallel lines with a periodicity of 3 nm are found. This is attributed to the mesostructure of CMK-3 where carbon rods fixed in a parallel position form a *p6mm* hexagonal lattice. The mesopores are formed among the carbon rods. Shadows of around 2.5–4.5 nm in size can be found along the parallel lines, which are attributed to Li_2MnSiO_4 crystallites. These observations strongly suggest that the oxide crystallites

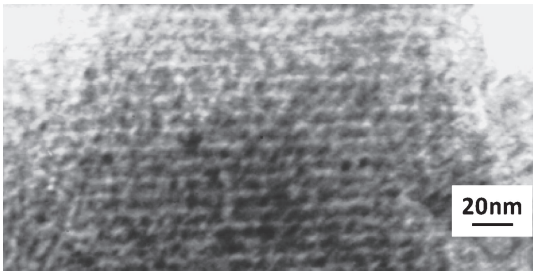

Figure 1. TEM image of LMS0.5@CMK-3.

 © 2011 The Chemical Society of Japan

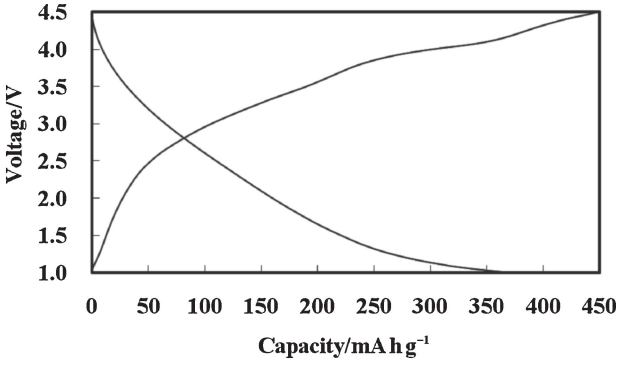

Figure 2. Charge and discharge curves of LMS0.5@CMK-3 in the second cycle. The data were recorded at 0.1 C and at room temperature.

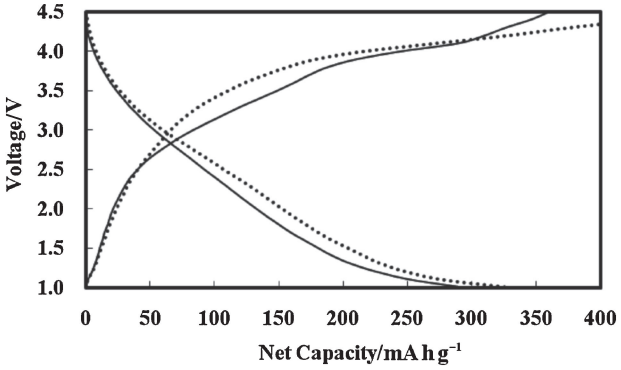

Figure 3. Net charge and discharge curves of Li_2MnSiO_4 in an LMS0.5@CMK-3 electrode in the first (dots) and the second (solid) cycles calculated from those obtained for LMS0.5@CMK-3 and CMK-3 recorded at 0.1 C and at room temperature.

are grown mainly in the pores of CMK-3. The shadow forms dots rather than lines, suggesting that the oxide grew as particles rather than rods in the case of LMS0.5@CMK-3.

The X-ray diffraction pattern of LSM0.5@CMK-3 is depicted in Figure S4.[28] Most of the peaks are attributed to Li_2MnSiO_4, and the relative intensities of the peaks agree with the known patterns for its bulk oxide, though the peak widths are broadened. This peak broadening is possibly due to the small crystalline sizes. Some peaks that can be assigned to MnO are also found, implying the presence of manganese(II) oxide as the major impurity. On the other hand, SEM-EDX image of the solid implies that the spatial distribution of elements is unform as shown in Figure S5.[28]

The galvanostatic charge–discharge curves of the second cycle are plotted in Figure 2. The capacity apparently reaches ca. 360 mA h g^{-1}, a value larger than that expected theoretically. The large capacity is well kept even after 10 cycles (see ESI). However, both the charge and the discharge processes are inevitably influenced by direct electrochemical reactions of the surface of CMK-3 that can be in contact with the electrolyte. Namely, CMK-3 must work as an electrode as well as an electroconductive framework, like electrodes formed from conductive carbon. Although it is difficult to know how the charge–discharge process occurs on the carbon surface in LMS*x*@CMK-3, a reduction of pore volume by the insertion of Li_2MnSiO_4 into the mesopores is approximately proportional to the loss of surface area of the framework carbon, considering that the periodicity of CMK-3 is two-dimensional and assuming that the mesopores are well developed (i.e., that the aspect ratio is large). Using the factors calculated from the pore volumes of CMK-3 and LMS0.5@CMK-3 (1.17 and 0.596 mL g^{-1}, respectively), then net charge–discharge curves are obtained as shown in Figure 3. A significant change appears in the discharge curve after the first cycle, as with other Li_2MnSiO_4 electrodes reported to date, which has often been attributed to a transition from a crystalline structure into an amorphous state.[21] In the second cycle, the capacity in the charge process exceeds 360 mA h g^{-1}, while that in the discharge reaction reaches 300 mA h g^{-1}. These capacities are comparable to the values that are expected from the electrochemical reaction of $MnSiO_4 + 2Li^+ + e \rightarrow Li_2MnSiO_4$, 333.14 mA h g^{-1} Li_2MnSiO_4. This agreement suggests that all of the lithium cations are involved in the charge–discharge reactions. The small excess that is observed in the Li^+ charge capacity can possibly be attributed to an electrochemical reaction at the interface between Li_2MnSiO_4 and carbon. The large capacity, equivalent to the reaction with two Li^+ per Li_2MnSiO_4, is probably due to a shortening of the Li^+ path during the electrode reactions caused by a decrease in particle size into several nm. Furthermore, since mesoporous carbon CMK-3 is electroconductive,[27] the low intrinsic conductivity of Li_2MnSiO_4 can also be compensated by the decrease in particle size.

Substantial deformations of the charge and discharge curves between the first and second cycles can be observed in Figure 3. These changes have commonly been found in the measurement of Li_2MnSiO_4 and have been attributed to a degradation of the crystal structure.[8] A plateau at 4.0 V in the charge process becomes clear in the second cycle. This feature corresponds to the two $Mn^{2+/3+}$ and $Mn^{3+/4+}$ redox couples. No clear plateau appears during the discharge, which is in agreement with other observations for electrodes composed of much larger oxide particles.[8,16,20]

Even if the net capacity is calculated using the whole charge–discharge curve of CMK-3 with the identical weight contained in LMS0.5@CMK-3, we obtain a value exceeding 225 mA h g^{-1} for the second cycle. This is still much larger than that expected for the electrochemical process $LiMnSiO_4 + Li^+ + e \rightarrow Li_2MnSiO_4$ (166.57 mA h g^{-1} Li_2MnSiO_4). In this calculation, the influence of the carbon surface is clearly overestimated, though the net capacity is still comparable with the largest capacity reported for Li_2MnSiO_4 coated with carbon (220 mA h g^{-1} for an electrode composed of ca. 20 nm Li_2MnSiO_4 particles coated with a thin carbon layer, as measured at 323 K at a rate of 0.02 C).[21]

The above results imply that the capacity of the Li^+ charge–discharge cycle is much larger when using an electrode formed from Li_2MnSiO_4 nanoparticles filling the periodically ordered mesopores of CMK-3 than when using an electrode composed of Li_2MnSiO_4 particles coated with an "ill-defined" carbon layer. Two structural features can be pointed out in LMS*x*@CMK-3 electrodes: a small particle size (2.5–4.5 nm) and a uniform carbon framework. Further study into this composite electrode is underway in which the structure of LMS*x*@mesoporous carbon electrodes are systematically changed.

 © 2011 The Chemical Society of Japan

The authors thank the New Energy and Industrial Technology Development Organization (NEDO) for its financial support. They also thank Prof. Toru Wakihara (YNU) for kind support in the observation by transmission microscopy.

References and Notes

1 R. Dominko, M. Bele, M. Gaberšček, A. Meden, M. Remškar, J. Jamnik, *Electrochem. Commun.* **2006**, *8*, 217.
2 V. V. Politaev, A. A. Petrenko, V. B. Nalbandyan, B. S. Medvedev, E. S. Shvetsova, *J. Solid State Chem.* **2007**, *180*, 1045.
3 A. Nytén, A. Abouimrane, M. Armand, T. Gustafsson, J. O. Thomas, *Electrochem. Commun.* **2005**, *7*, 156.
4 A. Nytén, S. Kamali, L. Häggström, T. Gustafsson, J. O. Thomas, *J. Mater. Chem.* **2006**, *16*, 2266.
5 A. Nytén, M. Stjerndahl, H. Rensmo, H. Siegbahn, M. Armand, T. Gustafsson, K. Edström, J. O. Thomas, *J. Mater. Chem.* **2006**, *16*, 3483.
6 C. Lyness, B. Delobel, A. R. Armstrong, P. G. Bruce, *Chem. Commun.* **2007**, 4890.
7 R. Dominko, M. Bele, A. Kokalj, M. Gaberscek, J. Jamnik, *J. Power Sources* **2007**, *174*, 457.
8 Y.-X. Li, Z.-L. Gong, Y. Yang, *J. Power Sources* **2007**, *174*, 528.
9 J. Moskon, R. Dominko, R. Cerc-Korosec, M. Gaberscek, J. Jamnik, *J. Power Sources* **2007**, *174*, 683.
10 R. Dominko, *J. Power Sources* **2008**, *184*, 462.
11 D. Ensling, M. Stjerndahl, A. Nytén, T. Gustafsson, J. O. Thomas, *J. Mater. Chem.* **2009**, *19*, 82.
12 W. Liu, Y. Xu, R. Yang, *J. Alloys Compd.* **2009**, *480*, L1.
13 P. Ghosh, S. Mahanty, R. N. Basu, *J. Electrochem. Soc.* **2009**, *156*, A677.
14 I. Belharouak, A. Abouimrane, K. Amine, *J. Phys. Chem. C* **2009**, *113*, 20733.
15 V. Aravindan, K. Karthikeyan, S. Ravi, S. Amaresh, W. S. Kim, Y. S. Lee, *J. Mater. Chem.* **2010**, *20*, 7340; V. Aravindan, K. Karthikeyan, K. S. Kang, W. S. Yoon, W. S. Kim, Y. S. Lee, *J. Mater. Chem.* **2011**, *21*, 2470.
16 C. Deng, S. Zhang, B. L. Fu, S. Y. Yang, L. Ma, *Mater. Chem. Phys.* **2010**, *120*, 14.
17 N. Yabuuchi, Y. Yamakawa, K. Yoshii, S. Komaba, *Electrochem.* **2010**, *78*, 363.
18 X. Huang, X. Li, H. Wang, Z. Pan, M. Qu, Z. Yu, *Solid State Ionics* **2010**, *181*, 1451.
19 R. Dominko, I. Arčon, A. Kodre, D. Hanžel, M. Gaberšček, *J. Power Sources* **2009**, *189*, 51.
20 V. Aravindan, S. Ravi, W. S. Kim, S. Y. Lee, Y. S. Lee, *J. Colloid Interface Sci.* **2011**, *355*, 472.
21 T. Muraliganth, K. R. Stroukoff, A. Manthiram, *Chem. Mater.* **2010**, *22*, 5754.
22 J. Lee, J. Kim, T. Hyeon, *Adv. Mater.* **2006**, *18*, 2073; P. Simon, Y. Gogotsi, *Nat. Mater.* **2008**, *7*, 845; A.-H. Lu, F. Schüth, *Adv. Mater.* **2006**, *18*, 1793; C. Liang, Z. Li, S. Dai, *Angew. Chem., Int. Ed.* **2008**, *47*, 3696; Y. Wan, Y. Shi, D. Zhao, *Chem. Mater.* **2008**, *20*, 932; B. Sakintuna, Y. Yürüm, *Ind. Eng. Chem. Res.* **2005**, *44*, 2893; M. Kruk, B. Dufour, E. B. Celer, T. Kowalewski, M. Jaroniec, K. Matyjaszewski, *J. Phys. Chem. B* **2005**, *109*, 9216; C. Liu, F. Li, L.-P. Ma, H.-M. Cheng, *Adv. Mater.* **2010**, *22*, E28.
23 A. Vinu, T. Mori, K. Ariga, *Sci. Technol. Adv. Mater.* **2006**, *7*, 753.
24 H. Yang, D. Zhao, *J. Mater. Chem.* **2005**, *15*, 1217.
25 A. Vinu, M. Miyahara, V. Sivamurugan, T. Mori, K. Ariga, *J. Mater. Chem.* **2005**, *15*, 5122.
26 S. H. Joo, S. J. Choi, I. Oh, J. Kwak, Z. Liu, O. Terasaki, R. Ryoo, *Nature* **2001**, *412*, 169.
27 Y. Oda, K. Fukuyama, K. Nishikawa, S. Namba, H. Yoshitake, T. Tatsumi, *Chem. Mater.* **2004**, *16*, 3860.
28 Supporting Information is available electronically on the CSJ-Journal Web site, http://www.csj.jp/journals/chem-lett/index.html.

 © 2011 The Chemical Society of Japan